Evidence for Nucleon-Resonance Excitation in ω -Meson Photoproduction

Article *in* Physical Review Letters · May 2006

DOI: 10.1103/PhysRevLett.96.132003 · Source: PubMed

14 authors, including:

Jassem Ajaka
Lebanese University Council
31 PUBLICATIONS **353** CITATIONS
SEE PROFILE

Sylvain Bouchigny
Atomic Energy and Alternative Energies Commission
236 PUBLICATIONS **3,784** CITATIONS
SEE PROFILE

Lionel Fichen
French National Centre for Scientific Research
16 PUBLICATIONS **188** CITATIONS
SEE PROFILE

Alexander Mushkarenkov
Russian Academy of Sciences
119 PUBLICATIONS **1,290** CITATIONS
SEE PROFILE

Evidence for Nucleon-Resonance Excitation in ω-Meson Photoproduction

J. Ajaka,[1] Y. Assafiri,[1] S. Bouchigny,[1] J. P. Didelez,[1] L. Fichen,[1] M. Guidal,[1] E. Hourany,[1,*] V. Kouznetsov,[2] R. Kunne,[1] A. N. Mushkarenkov,[2] V. Nedorezov,[2] N. Rudnev,[2] A. Turinge,[3] and Q. Zhao[1,4]

[1]*IN2P3, Institut de Physique Nucléaire, 91406 Orsay, France*
[2]*Institute for Nuclear Research, 60th October Anniversary Prospect 7a, 117 312 Moscow, Russia*
[3]*I. Kurchatov Institute of Atomic Energy, Kurchatov Square Bldg. 1, 123182, Moscow, Russia*
[4]*Department of Physics, University of Surrey, Guildford GU2 7XH, United Kingdom*

(Received 24 January 2006; published 7 April 2006)

The photoproduction of the ω meson has been studied at GRAAL from threshold up to a photon energy of 1.5 GeV. The differential cross sections and beam asymmetries have been measured precisely at all angles. The total cross section is also obtained. Systematic enhancements of the differential cross section at large angles and nonzero beam asymmetries at intermediate angles provide clear evidence for s- and u-channel resonant processes. The data are compared to the results of hadron and quark models.

DOI: 10.1103/PhysRevLett.96.132003 PACS numbers: 13.60.Le, 13.88.+e, 14.40.Cs

The quark model predicts a large number of nucleon resonances which have not yet been observed [1]. Since the most used reaction for their study was pion-nucleon scattering, one could infer that these so-called ''missing resonances'' may couple weakly to this channel. In this Letter we report on the study of the nucleon resonances via ω meson photoproduction on the proton. This channel is interesting for several reasons. First, there is no nucleon resonance well-established decaying by ω emission. Second, the threshold of ω photoproduction lies in the third resonance region, which is less explored than the first two. Third, from the sparse data in the literature [2–4] and a new generation experiment [5], evidence for resonance excitations in $\gamma p \rightarrow \omega p$ is still not obvious. Because of the t-channel dominance at forward angles, a backward angle measurement is needed to pin down decisive signals for resonance excitations. Since the ω meson has isospin zero, only the isospin-1/2 nucleon resonances can couple to the ωN channel. This simplifies the interpretation of the data because there is no contribution from isospin-3/2 resonances. Also, we can measure Σ beam asymmetries and it is known that polarization observables are generated by interference terms and can therefore reveal small contributions. Finally, theoretical models are available for the interpretation of the results [6–11].

At GRAAL, a tagged and linearly polarized photon beam is available to study ω production from threshold (1.1 GeV) up to 1.5 GeV [12]. The beam is produced by backscattering a laser beam on the electron beam (6.04 GeV and 200 mA) in the European Synchrotron Radiation Facility (ESRF) ring. A UV line of the laser is used, which produces a photon beam with a flat energy spectrum from 0.6 up to 1.5 GeV. The beam is linearly polarized with a rate P, deduced from QED calculation, ranging from 86% at threshold to 98% at the maximum energy. The large acceptance detector allows the detection of the ω meson by its main decays into $\pi^+\pi^-\pi^0$ and $\pi^0\gamma$ with branching ratios of 89.1% and 8.7%, respectively. In the central part of the detector, for $25 \leq \theta \leq 155$ degrees, a barrel of 32 scintillators provides a veto for a bismuth germanate (BGO) ball calorimeter of 32 sectors and 15 crowns. In the frontal part, for $1 \leq \theta \leq 25$ degrees, there is a double wall of scintillators backed by a lead-scintillator shower wall [12]. A liquid hydrogen target of 6 cm is used.

In the analysis of $\gamma p \rightarrow p\omega$ with $\omega \rightarrow \pi^0\gamma$, three photons are requested in the BGO ball and one charged particle in the central or the forward part. For $\gamma p \rightarrow p\omega$ with $\omega \rightarrow \pi^+\pi^-\pi^0$, two photons are requested in the BGO ball and three charged particles in the central or the forward part, with at least one charged particle detected in the central part. The detection of photons is restricted to the BGO ball in order to take advantage of its energy resolution ($\leq 3\%$) [13] in the detection of electromagnetic showers, which is much better than the resolution of the forward shower wall [14]. For the ω three pion decay all the phase space is explored and the branching ratio is high. This channel is therefore preferred for the quantitative study, while the decay into $\pi^0\gamma$ is analyzed for consistency and checking.

Concerning the identification of the $\gamma p \rightarrow p\omega$ with $\omega \rightarrow \pi^+\pi^-\pi^0$, for each event the four energy and momentum conservation laws were used. In these equations the known quantities are the direction and energy of the incident photon given by the tagging system and of the π^0-meson reconstructed from the BGO calorimeter. The θ and ϕ angles of the proton and the 2 charged pions are also known from the cellular geometry of the detector. Solving 3 out of the 4 equations, one deduces the magnitude of the momenta p of the 3 charged particles. By combining for each particle the deduced p and the measured ΔE from the barrel or the time of flight (TOF) from the double wall, and looking at the location in a calibrated bidimensional ($\Delta E \times p$) or (TOF $\times p$) plot, the type of particle can be identified. The fourth equation is used to determine the best vertex position along the axis of the target, which improves the determination of the θ-angles of the particles detected

in the central detector and consequently the resolution of the invariant mass of the 3 pions. At this stage of analysis, the selected events are pure $\gamma p \to p\pi^+\pi^-\pi^0$ events. They originate from 3 possible reactions: (i) $\gamma p \to p\omega$ with $\omega \to \pi^+\pi^-\pi^0$, (ii) $\gamma p \to p\eta$ with $\eta \to \pi^+\pi^-\pi^0$, and (iii) the 4-body phase space reaction $\gamma p \to p\pi^+\pi^-\pi^0$. The events of reaction (ii) can be completely removed by a cut around the invariant mass of the η. Only the events of the nonresonant 4-body reaction (iii) constitute a real problem and the only way to minimize their contribution is the decomposition of the invariant mass spectrum of 3 pions into a sharp peak (FWHM $\approx$ 35 MeV) from the ω meson and a smooth background from the 4-body channel under the peak. The shapes of the peak and of the background are taken from simulations. Within the reaction kinematics, the background-to-peak height ratio varies from 10% to 30% and the decomposition error from 3% to 8%.

This method of decomposition is applied to each group of events after having sorted the data according to the kinematics of the 2-body reaction $\gamma p \to p\omega$. In order to extract the differential cross section $d\sigma/d(|t|)$ for $\gamma p \to p\omega$, where t is the Mandelstam variable, the events are sorted into 300 kinematical intervals, corresponding to 10 bins in E_γ and 30 bins in t. To extract the beam asymmetry Σ as a function of E_γ and the scattering angle $\Theta_\omega^{\text{c.m.}}$ (c.m. referring to the center-of-mass frame), the data are sorted, for each of the vertical and horizontal beam polarizations, into 336 kinematical intervals, corresponding to 4 bins in E_γ, 7 bins in $\Theta_\omega^{\text{c.m.}}$, and 12 bins in the azimuthal angle ϕ_ω. After these decompositions, the number of ω events obtained in each kinematical interval needs to be corrected by the detection efficiency using the simulation calculation.

The simulation calculation uses the code LAGGEN of GRAAL which consists of an event generator followed by tracking with GEANT3 from the CERN library. In the event generator, we use an energy spectrum with Compton shape for the gamma beam and a differential cross section for ω meson photoproduction based on a 2-body phase space. As to the distribution of the 3 pions from ω decay, a phase space distribution in the rest frame of ω, and a distribution induced by a double polarization (beam-vector meson) [15,16] are used. With the simulation calculation, an efficiency table $\epsilon(E_\gamma, |t|)$ is calculated. An essential check is that the values in the table do not change significantly (with respect to the statistical errors) between the two types of distributions of the 3 pions in the rest frame of ω. Since the whole phase space is covered by the acceptance of the detector, the cross sections are extracted without extrapolation, requiring only efficiency corrections, (average efficiency $\approx$ 0.10).

In order to extract the beam asymmetry $\Sigma(E_\gamma, \Theta_\omega^{\text{c.m.}})$, the method used previously in single pseudoscalar meson photoproduction is applied [12,17–19]. For ω events falling into each kinematical interval $(E_\gamma, \Theta_\omega^{\text{c.m.}})$, the distribution of $N(\phi)$ is plotted, where ϕ is the angle between the production plane of ω meson and the horizontal plane. This gives two distributions $N^V(\phi)$ and $N^H(\phi)$ corresponding to the beam vertical and horizontal polarization directions, respectively. The ratio $R(\phi) = 2N^V(\phi)/[N^V(\phi) + N^H(\phi)]$ is fitted by the expression $1 + P\Sigma\cos(2\phi)$, from which the beam asymmetry Σ is deduced. Another essential check with the simulation is that $R(\phi)$ does not significantly depend on the detection efficiency for the above mentioned two types of distributions of the decay products of the ω in its rest frame. The success of these two checks comes from the averaging out due to the large number of possible directions of the ω decay products spread through the detector acceptance (5 independent kinematical variables in the ω rest frame).

The GRAAL data of the $\gamma p \to p\omega$ reaction with $\omega \to \pi^+\pi^-\pi^0$, corresponding to a total of 86 000 pure ω events, are displayed in Figs. 1–4, together with some of the existing world data.

Recently, for the search of the missing resonances, several theoretical models have been developed in ω meson photoproduction and were particularly interested in the beam asymmetry results from the GRAAL data. All these models took the nonresonant amplitudes of the ω channel

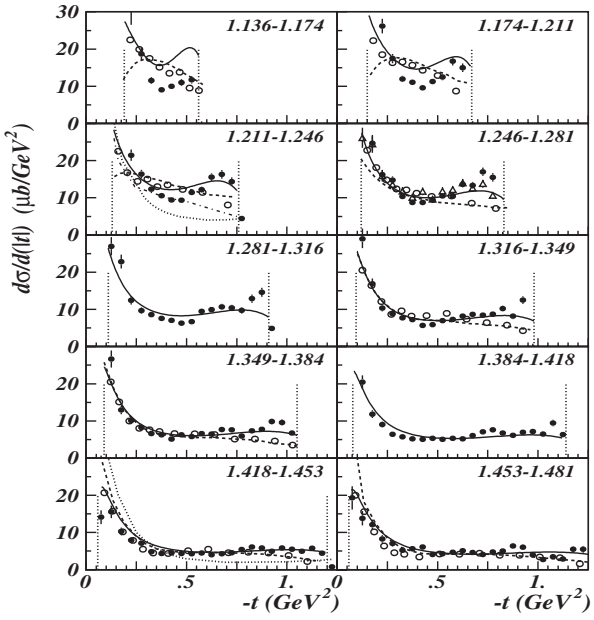

FIG. 1. Differential cross sections of $\gamma p \to p\omega$. The GRAAL data for $\omega \to \pi^+\pi^-\pi^0$ are shown as solid circles. For a consistency check of the angular distribution pattern, the GRAAL data for the $\omega \to \pi^0\gamma$ channel have been plotted with open triangles at the E_γ = 1.246–1.281 GeV bin. The vertical dashed lines indicate the kinematical limits in $-t$. The calculations of Zhao are solid lines. The open circles are data from Ref. [5]. The dashed lines are the calculation of Penner and Mosel [10]. The two dotted curves are calculations of Oh *et al.* [8] and the dot-dashed curve, of Titov and Lee [9].

from previous investigations at higher energies and calculated the resonant amplitudes from effective Lagrangians. Titov and Lee took the $N^* \to \gamma N$ and $N^* \to \omega N$ coupling constants fixed by the empirical helicity amplitudes and the vector-meson dominance model [9]. Penner and Mosel, analyzing the photon- and pion-induced reactions developed a unitary coupled-channel Lagrangian including the ω production channel [10,11]. Zhao *et al.*, within a quark model approach built on the SU(6) ⊗ O(3) basis, used the quark vector-meson coupling [6,7] and resonance contributions from the s and u -channels. Oh *et al.* [8] took the resonance parameters from a quark model by Capstick and Roberts [20].

In Fig. 1, the differential cross section $d\sigma/d(|t|)$ is shown as a function of $-t$ for 10 beam energy bins. The experimental data are plotted as dots with statistical error bars. The systematic errors, not shown in the figure, come from the flux determination (3%) and the background subtraction [21]. The data exhibit, at low $|t|$ values, a fast decrease which is characteristic of t-channel exchanges [22] and, at high $|t|$, a cross-section enhancement which is the signature of s- and u-channel transitions. The model of Zhao *et al.* [6,7], plotted in a continuous line, satisfactorily reproduces the trends of our data.

We show in the same figure (plotted in open circles) some of the results of Barth *et al.* [5] which match approximately our beam energy bins, together with the calculations of Penner and Mosel (plotted in a dashed line), which included in their database the data of Barth *et al.* [10]. These results do not exhibit the characteristic pattern seen in our results, especially near threshold. Nevertheless, they show at high $|t|$ values a clear deviation from the exponential decrease of the t-channel exchange. Such a deviation is also confirmed by the two dotted curves given by the model of Oh *et al.* [8] and the dot-dashed curve given by the model of Titov.

In Fig. 2, the total cross section is shown. The GRAAL data (solid dots), are obtained by the integration of the differential cross sections given in Fig. 1. The error bars come mainly from the uncertainty at the limits of the integration. The systematic error of 5% is not shown. Similar to the previous existing data (shown with empty symbols), a strong rise at threshold is seen in GRAAL data. Moreover, a bump structure appears near threshold before the total cross section levels off to a value of $\approx 7.5\mu b$ at 1.45 GeV. The model of Zhao *et al.* (solid line) satisfactorily reproduces the GRAAL data, and, in particular, among its different transition processes (shown in the figure) the resonant term is dominant near threshold and remains sizeable up to $E_\gamma = 2$ GeV. The same structure is also seen in the results of Barth *et al.* [5] plotted in open circles and in the calculation of Penner and Mosel [10] (shown by the heavy dashed line), where the enhancement near threshold is attributed by the authors to $P_{11}(1710)$ and $P_{13}(1900)$ contributions.

In Figs. 3 and 4 the beam asymmetry Σ data are presented with dots as a function of $\Theta_\omega^{\text{c.m.}}$ for 4 bins of beam energy, together with the predictions or the fit results of the various theoretical models. The errors on the experimental values of Σ come from fitting the $R(\phi)$ distribution with the expression $1 + P\Sigma\cos(2\phi)$. The systematic errors, not shown in the figure, come from the polarization (3%) and from the background subtraction [21]. The experimental values of Σ are found negative and large at intermediate angles. They are the convincing signal of s- and u-channel transitions, particularly the excitation of nucleonic resonances. Because of helicity conservation of the dominant pion exchange and small diffractive contribution (e.g., Pomeron exchange) near threshold, the beam asymmetry

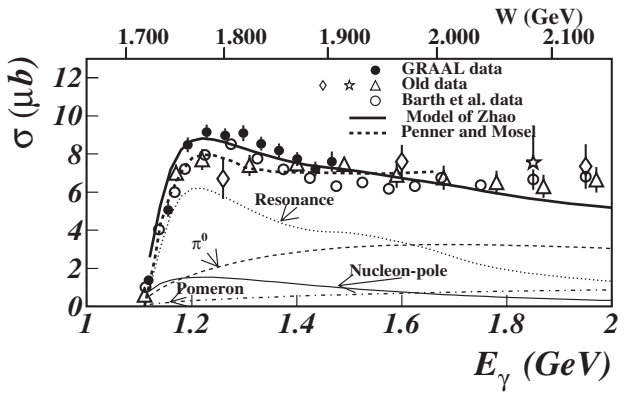

FIG. 2. Total cross section of $\gamma p \to p\omega$. The GRAAL data are shown as solid circles. The old data are: diamonds from Ref. [2], stars from Ref. [3], triangles from Ref. [4], and open circles from Ref. [5]. The calculations by Zhao are shown with several lines: solid for the full calculation, and other line types for contributing terms. The thicker dashed line is the calculation of Penner and Mosel [10].

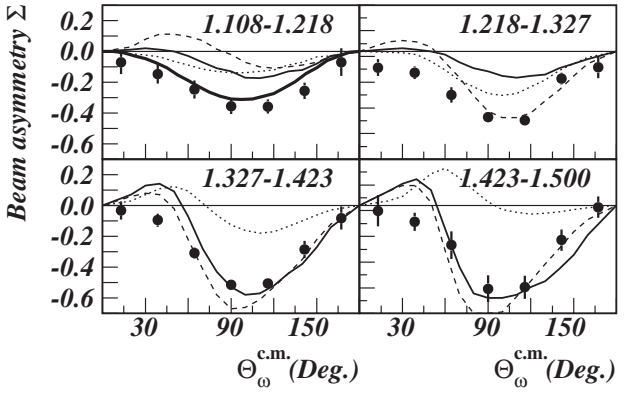

FIG. 3. Beam asymmetry of $\gamma p \to p\omega$ for 4 bins of beam energy. The GRAAL data are shown as solid circles. The thick line is the calculation of Titov *et al.* at 1.175 GeV [9]. The thin continuous and dashed lines are the predictions of Penner and Mosel calculation [10] for positive and negative signs of the coupling $g_{\omega\rho\pi}$. The dotted lines are the calculation of Shklyar *et al.* [11].

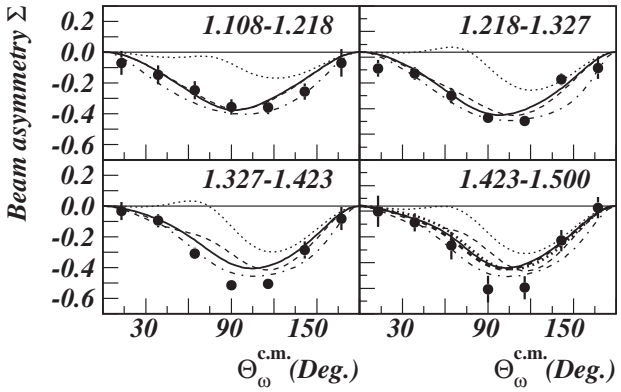

FIG. 4. Beam asymmetry of $\gamma p \to p\omega$. The same GRAAL data as in Fig. 3. The calculations by Zhao are given with different lines: solid line for full calculation; dashed line for no $D_{13}(1520)$ contribution; dotted line for no $P_{13}(1720)$; and dot-dashed line for no $F_{15}(1680)$. At the 1.423–1.500 GeV bin, the heavy-dashed line is for no $F_{15}(2000)$ and the heavy-dotted line for no $P_{13}(1900)$.

Σ would be vanishing without the helicity-violating s- and u-channel transitions, particularly the excitation of resonances.

In Fig. 3, the results of hadronic models are shown. The thick continuous line represents the result of Titov *et al.* calculated at 1.175 [9]. The authors attribute the sizeable negative asymmetry to the interference between the nonresonant and resonant amplitudes. The dominant resonant contribution comes from the excitation of $F_{15}(1680)$ state, whereas smaller contributions come from $D_{13}(1520)$, $S_{11}(1650)$, and $P_{13}(1720)$ states. Also in the same figure, are plotted the predictions of the Penner and Mosel model [10], in thin continuous and dashed lines for the positive and negative sign of the coupling $g_{\omega\rho\pi}$, respectively. The predictions agree better with the data at higher energy. From the figure, no decisive conclusion can be drawn to extract the sign of the coupling. The authors have found in their calculation of ω photoproduction a clear dominant contribution from the $P_{11}(1710)$ and smaller ones from $P_{13}(1720)$ and $P_{13}(1900)$ states. The calculation by Shklyar *et al.* [11] using the model of Penner and Mosel but allowing several resonances to contribute in ω production is shown in dotted lines. Big changes in shape and size are seen, rendering a poorer agreement with the experimental results.

In Fig. 4, our beam asymmetry data are presented with the interpretation by Zhao *et al.* who give, with solid lines, the full calculation results and, with other line types, the results when one single resonance is switched off (keeping the relative strengths of the remaining resonances as imposed by the quark model). So, some of the resonances, e.g., $D_{13}(1520)$, $P_{13}(1720)$, $F_{15}(1680)$, are found to play an indispensable role, and some effects due to the $F_{15}(2000)$ are also seen. In particular, the model suggests that $P_{13}(1720)$ plays an important role near threshold despite a small branching ratio 0.002 while the $P_{13}(1900)$ and $F_{15}(2000)$ have sizeable branching ratios, 0.1 and 0.4, but small contributions to the cross section.

To summarize, the photoproduction of the ω meson has been studied at GRAAL from threshold up to $E_\gamma = 1.5$ GeV. Strong signals indicating resonance excitations are observed in this channel via the precise measurements over a wide angular range of the differential cross sections and, for the first time, of the beam asymmetries.

The comparison of these data to hadron and quark model results shows that contributions from on-shell and off-shell resonances are both required. In particular, two poorly known resonances, $P_{13}(1900)$ and $F_{15}(2000)$, are found to have sizeable decay branching ratios into ωN. It is expected that the present data will trigger the improvement of the existing models.

*Electronic address: hourany@ipno.in2p3.fr

[1] S. Capstick and W. Roberts, Prog. Part. Nucl. Phys. **45**, S241 (2000).
[2] R. Erbe *et al.* (ABBHHM Collaboration), Phys. Rev. **175**, 1669 (1968).
[3] W. Struczinski *et al.*, Nucl. Phys. **B108**, 45 (1976).
[4] F. J. Klein, Ph.D. thesis, University of Bonn, Bonn-IR-96-008, 1996; πN Newsletter **14**, 141 (1998).
[5] J. Barth *et al.*, Eur. Phys. J. A **18**, 117 (2003).
[6] Q. Zhao, Z. Li, and C. Bennhold, Phys. Lett. B **436** 42 (1998); Phys. Rev. C **58**, 2393 (1998).
[7] Q. Zhao, Phys. Rev. C **63**, 025203 (2001).
[8] Y. Oh, A. I. Titov, and T. S. H. Lee, Phys. Rev. C **63**, 025201 (2001).
[9] A. I. Titov and T. S. H. Lee, Phys. Rev. C **66**, 015204 (2002).
[10] G. Penner and U. Mosel, Phys. Rev. C **66**, 055212 (2002).
[11] V. Shklyar, H. Lenske, U. Mosel, and G. Penner, Phys. Rev. C **71**, 055206 (2005).
[12] J. Ajaka *et al.*, Phys. Rev. Lett. **81**, 1797 (1998).
[13] F. Ghio *et al.*, Nucl. Instrum. Methods Phys. Res., Sect. A **404**, 71 (1998).
[14] V. Kouznetsov *et al.*, Nucl. Instrum. Methods Phys. Res., Sect. A **487**, 396 (2002).
[15] K. Schilling *et al.*, Nucl. Phys. **B15**, 397 (1970).
[16] J. Ballam *et al.*, Phys. Rev. D **7**, 3150 (1973).
[17] J. Ajaka *et al.*, Phys. Lett. B **475**, 372 (2000).
[18] F. Renard *et al.*, Phys. Lett. B **528**, 215 (2002).
[19] O. Bartalini *et al.*, Phys. Lett. B **544**, 113 (2002).
[20] S. Capstick and W. Roberts, Phys. Rev. D **49**, 4570 (1994).
[21] Omega photoproduction data at GRAAL (to appear in Durham HEP Databases).
[22] B. Friman and M. Soyeur, Nucl. Phys. **A600**, 477 (1996).